STP 1543, 2014 / available online at www.astm.org / doi: 10.1520/STP154320120168

Kimberly Colas,[1] Arthur Motta,[2] Mark R. Daymond,[3] and Jonathan Almer[4]

Mechanisms of Hydride Reorientation in Zircaloy-4 Studied in Situ

Reference

Colas, Kimberly, Motta, Arthur, Daymond, Mark R., and Almer, Jonathan, "Mechanisms of Hydride Reorientation in Zircaloy-4 Studied in Situ," *Zirconium in the Nuclear Industry: 17th International Symposium*, STP 1543, Robert Comstock and Pierre Barberis, Eds., pp. 1107–1137, doi:10.1520/STP154320120168, ASTM International, West Conshohocken, PA 2014.[5]

ABSTRACT

Zirconium hydride platelet reorientation in fuel cladding during dry storage and transportation of spent nuclear fuel is an important technological issue. Using an in situ x-ray synchrotron diffraction technique, the detailed kinetics of hydride precipitation and reorientation can be directly determined while the specimen is under stress and at temperature. Hydrided Zircaloy-4 dogbone sheet samples were submitted to various thermo-mechanical schedules, while x-ray diffraction data was continuously recorded. Post-test metallography showed that nearly full hydride reorientation was achieved when the applied stress was above 210 MPa. In general, repeated thermal cycling above the terminal solid solubility temperature increased both the reoriented hydride fraction and the connectivity of the reoriented hydrides. The dissolution and precipitation temperatures were determined directly from the hydride diffraction signal. The diffraction signature

Manuscript received November 19, 2012; accepted for publication July 28, 2013; published online September 17, 2014.

[1]Dept. of Mechanical and Nuclear Engineering, Penn State Univ., University Park, PA 16802, United States of America (Corresponding author), e-mail: kimberly.colas@cea.fr. (Currently at CEA, French Atomic Energy Commission, DEN/DANS/DMN/SEMI/LM2E, Saclay, France, 91191.)

[2]Dept. of Mechanical and Nuclear Engineering, Penn State Univ., University Park, PA 16802, United States of America.

[3]Dept. of Mechanical and Materials Engineering, Queen's Univ., Kingston, ON K7L3N6, Canada.

[4]Advanced Photon Source, Argonne National Laboratory, Argonne, IL 60439, United States of America.

[5]ASTM 17th International Symposium on *Zirconium in the Nuclear Industry* on February 3–7, 2013 in Hyderabad, India.

of reoriented hydrides is different than that of in-plane hydrides. During cooling under stress, the precipitation of reoriented hydrides occurs at lower temperatures than the precipitation of in-plane hydrides, suggesting that applied stress suppresses the precipitation of in-plane hydrides. The analysis of the elastic strains determined by the shift in position of hydride and zirconium diffraction peaks allowed following of the early stages of hydride precipitation. Hydride particles were observed to start to nucleate with highly compressive strain. These compressive strains quickly relax to smaller compressive strains within 30°C of the onset of precipitation. After about half of the overall hydride volume fraction is precipitated, hydride strains follow the thermal contraction of the zirconium matrix. In the case of hydrides precipitating under stress, the strains in the hydrides are different in direction and trend. Analyses performed on the broadening of hydride diffraction peaks yielded information on the distribution of strains in hydride population during precipitation and cooldown. These results are discussed in light of existing models and experiments on hydride reorientation.

Keywords
zirconium hydrides, reorientation, synchrotron x-ray diffraction

Introduction

During service in light water reactors (LWRs) hydrogen atoms from the corrosion reaction and water radiolysis enter the zirconium alloy nuclear fuel cladding, where they precipitate as a brittle hydride phase [1]. For older alloys, such as Zircaloy-4, at the high burnup rates used in today's reactors, oxide layers as thick as 100 μm and hydrogen content up to 700 wt. ppm can be observed in the cladding [2,3]. The hydrogen precipitates as brittle hydride platelets of the δ-hydride phase (face-centered cubic, $ZrH_{\sim 1.66}$), which leads to a degradation of the cladding ductility [4,5]. Although other hydride phases, such as γ- or ε-hydrides have also been observed under certain conditions, they are less typical in reactor cladding [6,7]. The δ-hydride platelets are composed of thin plates, the stacking of which results in the observed orientation of the large macroscopic hydrides seen by metallography. This orientation depends on the texture, grain morphology, and thermal history of the material [8]. When precipitated under no applied stress in cladding material, hydrides tend to precipitate in the circumferential-axial plane. However, stress can significantly affect the orientation of these hydride platelets: when precipitated under sufficient stress (such as can be found in used fuel cladding because of fission gas pressure at temperature), hydride platelets can precipitate with a different orientation in which the hydride platelet normal is parallel to the loading direction [9]. Reorientation of these hydrides can lead to a severe embrittlement of the material, because hydride cracking can facilitate crack propagation through the cladding thickness. The conditions of high stress and high temperature, which could lead to hydride reorientation, could potentially be found during transportation and dry

storage of used nuclear fuel. Thus the understanding of the hydride reorientation mechanism is of significant importance for used nuclear fuel storage and disposition.

Previous studies on hydride reorientation performed with conventional metallography techniques have provided essential information on the threshold stresses for reorientation and influencing factors [9,10]. However, the study of the detailed mechanisms of nucleation and growth of reoriented hydrides and the fine structure of these particles is difficult with such techniques as they can only access the initial and final states. Recent in situ synchrotron experiments have shown the potential to study hydride dissolution and precipitation using synchrotron radiation in normal mechanical test specimen [11,12], and in samples with a stress concentration [13,14]. The in situ x-ray diffraction technique is used in this article to study the mechanisms of hydride nucleation and growth with and without applied stress. The hydride volume fraction, phase and strain states are continuously followed during dissolution and precipitation. Several samples with no reorientation and full reorientation and different levels of applied stresses are studied.

Experimental Procedures

MATERIAL AND SAMPLE PREPARATION

The material used in this study is cold-worked Zircaloy-4 sheet of 675-μm thickness furnished by Teledyne Wah-Chang. The as-received sheet was stress relieved for 2 h at 510°C under a vacuum of 10^{-3} Pa, resulting in a cold-worked stress-relieved (CWSR) state. The microstructure, texture and mechanical properties of this material are detailed in [5]. The zirconium grains are elongated in the rolling direction with an average grain size of 6 μm in the rolling direction, 4.5 μm in the transverse direction and 2.5 μm in the normal direction. The crystallographic texture of the sheet is similar to that seen in CWSR zirconium cladding as illustrated in **Fig. 1** [15]. The yield stress of this material tested at several temperatures is 5–10 % lower than that of cladding tube.

The samples are then hydrided using a gaseous charging technique as described in [11]. This technique starts by removal of the native oxide layer by acid etching followed by deposition of a thin nickel layer, which will act as a window for hydrogen atoms and prevent oxidation. After this step, the samples are heated to 450°C in a volume filled with a mixture of 88 % argon and 12 % hydrogen to introduce the hydrogen and held for 1 h at temperature then furnace cooled. The hydrogen content of the hydrided samples was systematically tested using hot vacuum extraction. The hydrogen contents of the samples in this study range from 150 to 300 wt. ppm.

Once the samples are hydrided, they are machined into small dogbone-shaped tensile specimens, the dimensions of which are presented in **Fig. 2**. It is important to note that the transverse direction (TD) is along the sample loading direction. The rolling direction (RD) is perpendicular to the gage section along the plane of the

FIG. 1 (*a*) Schematic representation of the texture directions in the sheet material used in this study; (*b*) {00.2} pole figure of the sheet material used in this study [5]; (*c*) schematic representation of the texture directions in typical cladding material; and (*d*) {00.2} pole figure of typical cladding material [30].

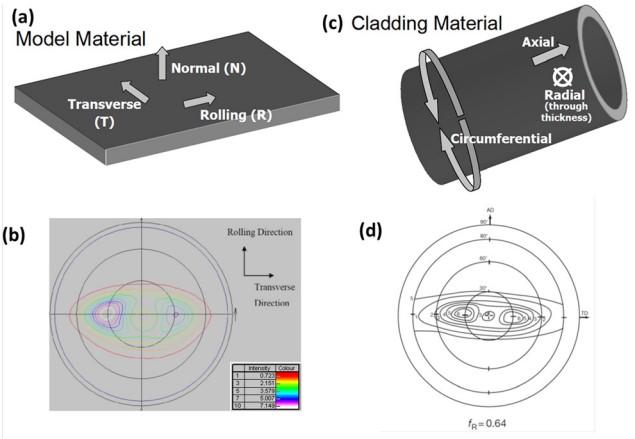

tensile specimen. The normal direction (ND) is perpendicular to the plane of the tensile specimen as illustrated in Fig. 1(*a*).

METALLOGRAPHY

Metallography is performed on the samples to observe the hydride microstructure. The samples are mounted in epoxy casts, polished to 1200 grit silicon carbide paper then etched for a few seconds in a solution of one volumetric part hydro-fluoric acid (HF), 10 parts nitric acid and 10 parts H_2O.

FIG. 2 Dogbone specimen geometry (sample thickness was 0.6 mm).

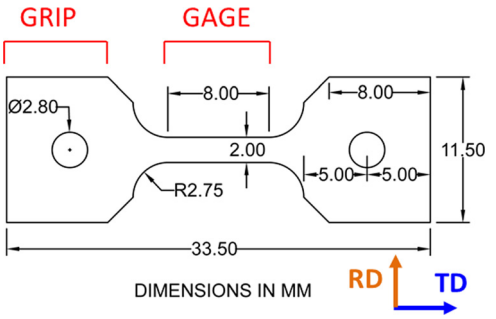

A small piece of the grip section of each sample is analyzed by metallography prior to any thermo-mechanical treatment, to determine the starting microstructure of the samples. Figure 3 shows optical micrographs of the ND-TD cross section of a typical starting hydride microstructure for different samples (labeled initial). The hydrides are mostly in-plane (i.e., platelets in the rolling-transverse plane). This is due both to the texture of the CWSR material, which presents many basal poles along the normal direction, perpendicular to the rolling-transverse plane and to the grain morphology. Hydride platelets typically precipitate in an orientation perpendicular to the basal pole because of the δ-hydride{111}// α-zirconium{0002} orientation relationship [16] and to the greater availability of grain boundaries of elongated grains in CWSR. After thermo-mechanical treatment at the Advanced Photon Source (APS) Synchrotron, the final hydride microstructure is also observed by metallography.

FIG. 3 Thermo-mechanical cycles and hydride microstructure before and after cycle: (*a*) sample with 294 wt. ppm of hydrogen, no applied stress, no reorientation; (*b*) sample with 246 wt. ppm of hydrogen, 160 MPa applied stress, no reorientation; and (*c*) sample with 192 wt. ppm, 240 MPa applied stress, and reorientation. Note: all micrographs are 500 μm in width.

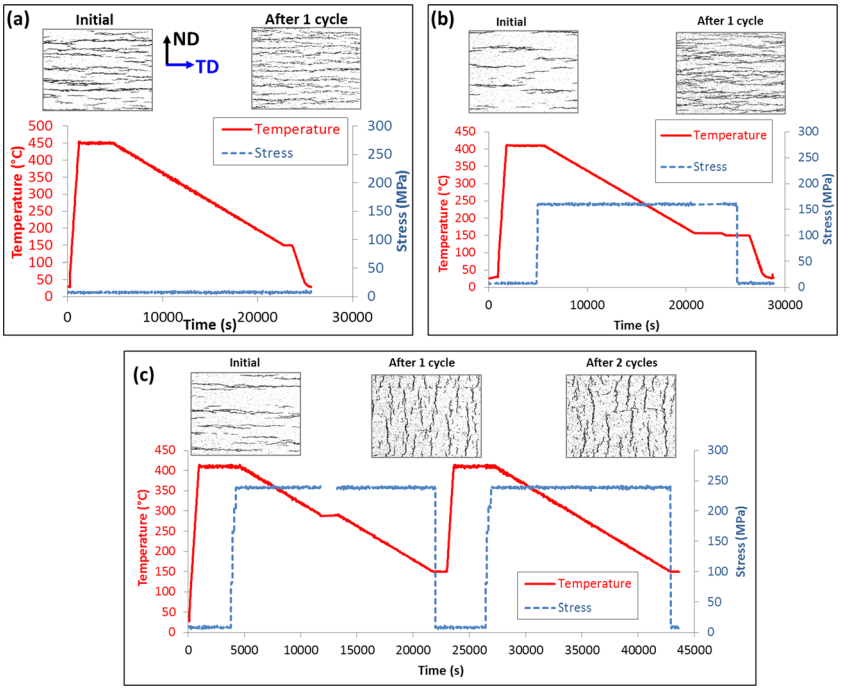

THERMO-MECHANICAL TREATMENT

Three different thermo-mechanical treatments are performed in this study on three different samples with similar levels of hydrogen. These thermo-mechanical treatments are shown for each sample in **Fig. 3**. The resulting hydride microstructure for each sample is also presented alongside the initial hydride microstructure in **Fig. 3**. In the treatment shown in **Fig. 3(*a*)** the sample is heated to full dissolution (450°C for 294 wt. ppm of hydrogen) and cooled without any applied load. In this case, the resulting hydride precipitates are mostly in-plane because of the initial texture. When a sample is heated to full dissolution and cooled with a low applied stress of 160 MPa, the final hydride microstructure is similar to the unstressed sample with most of the hydride platelets in the in-plane direction as can be seen in **Fig. 3(*b*)**. Finally, when a sample is heated until all the hydrides are dissolved and cooled under a high applied stress of 240 MPa, many hydrides reorient upon cooling, as seen in **Fig. 3(*c*)**. The radial hydride fraction (RHF) is calculated as a weighted average of hydride lengths where hydrides with an orientation between 0° and 40° to the transverse direction have a weight of 0, hydrides with an orientation between 40° and 65° have a weight of 0.5, and hydrides with an orientation of 65° to 90° have a weight of 1. More details on the methods of determining the RHF are described in [11]. Calculations based on image analysis of the hydrides as described in [11] show that the radial hydride fraction is approximately 60 % after one thermo-mechanical cycle. After two thermo-mechanical samples under 240 MPa, full reorientation is achieved (RHF ∼100 %). This indicates that the threshold stress for hydride reorientation for this CWSR Zircaloy-4 sample is between 160 and 230 MPa, which is consistent with literature results [17].

SYNCHROTRON X-RAY DIFFRACTION

X-ray diffraction (XRD) experiments were performed at beamline 1-ID at the Advanced Photon Source Synchrotron at Argonne National Laboratory. A detailed description of the transmission in situ diffraction technique and data analysis can be found in Refs 11 and 18. A 76-keV x-ray beam was used for these experiments, which allows transmission of the x rays through the sample thickness. The diffraction rings obtained are recorded onto a two-dimensional (2D) amorphous silicon detector allowing for some texture information to be measured. Diffraction data is recorded every 30 s during heating and cooling of the sample, allowing for the full hydride dissolution and precipitation kinetics to be studied.

The obtained diffraction rings are integrated along specific azimuthal directions (±5°). Families of planes perpendicular to the TD (direction of the applied stress) and perpendicular to the RD are studied in this experiment. Once integrated, the diffraction peaks are then fitted using software called General Structure Analysis System (GSAS) by iterative refinement of the peaks' shapes, intensities, and widths [19]. The peak shape chosen for these fits is a pseudo-Voigt shape, which is a convolution of Gaussian and Lorentzian shapes typically used for synchrotron diffraction peaks. The focus of this study is on the most intense hydride peak $\delta\{111\}$ and

its neighboring zirconium $\alpha\{10.0\}$ peak. The fitting error for the zirconium $\alpha\{10.0\}$ peak in a sample with 294 wt. ppm of hydrogen in the TD at room temperature is less than 1 % for the peak intensity and 0.002 % for the d-spacing (which corresponds to an error of about 0.01 millistrain for the zirconium elastic strain at room temperature). For the $\delta\{111\}$ hydride peak in the same sample at the same temperature, the error is less than 5 % for the peak intensity and 0.023 % for the d-spacing (which corresponds to an error of approximately 0.22 millistrain for the hydride elastic strain at room temperature). At 400°C where the hydride peak is much smaller, the error for the hydride peak become close to 45 % for the peak intensity and 0.36 % for the d-spacing (which corresponds to an error of approximately 3.5 millistrain for the hydride elastic strain at that temperature). The error for the fitting of the zirconium peak is the same at 400°C than at room temperature. The error bars were not represented for the zirconium and hydrides strain plots in **Figs. 7–13**, and for the Williamson-Hall plots in **Fig. 16** for the sake of clarity, but the error values mentioned above applicable to all observed samples. The value of the typical error in the Williamson-Hall plots in **Fig. 16** is equivalent to the scatter in the data.

Results

DISSOLUTION AND PRECIPITATION KINETICS

As described in Ref 11, the integrated intensity of the hydride peak $\delta\{111\}$ can be followed continuously during heating and cooling of the sample. The heating rate for the samples observed in this study is 25°C/min and the cooling rate is 1°C/min. As the sample is heated and hydrides dissolve, the hydride peak intensity decreases, reaching zero when full dissolution is achieved, which allows determination of dissolution temperature, T_d. When hydrides start to re-precipitate, the hydride peak reappears at the precipitation temperature T_p, and increases as more and more hydrides precipitate. After full re-precipitation is achieved, the hydride peak intensity is similar to the initial value for sample cooled under no applied stress. The determination of T_p and T_d was performed for several samples of various hydrogen contents, and the results compared with differential scanning calorimetry (DSC) determination [11]. **Figure 4** shows the experimental T_d and T_p compared to T_d and T_p curves determined in Une and Ishimoto [20] using differential scanning calorimetry [11]. The measured T_d and T_p for all samples correspond reasonably well with the temperatures measured in Ref 20 using DSC. The temperature hysteresis $(T_d - T_p)$ is also similar to that observed in Ref 20. The temperature error bars in this figure were determined by the heating/cooling rate and the time between acquisitions of successive diffraction patterns. The good agreement between the synchrotron XRD technique and the DSC techniques validates the use of the XRD technique to study hydride dissolution and precipitation.

It is interesting to note that when hydrides are already present at the start of cooling (full dissolution not achieved) the hysteresis disappears. This is illustrated in **Fig. 5**, which shows the hydride diffraction signal from a sample containing

FIG. 4 Dissolution and precipitation temperatures measured from in situ XRD compared to DSC [20].

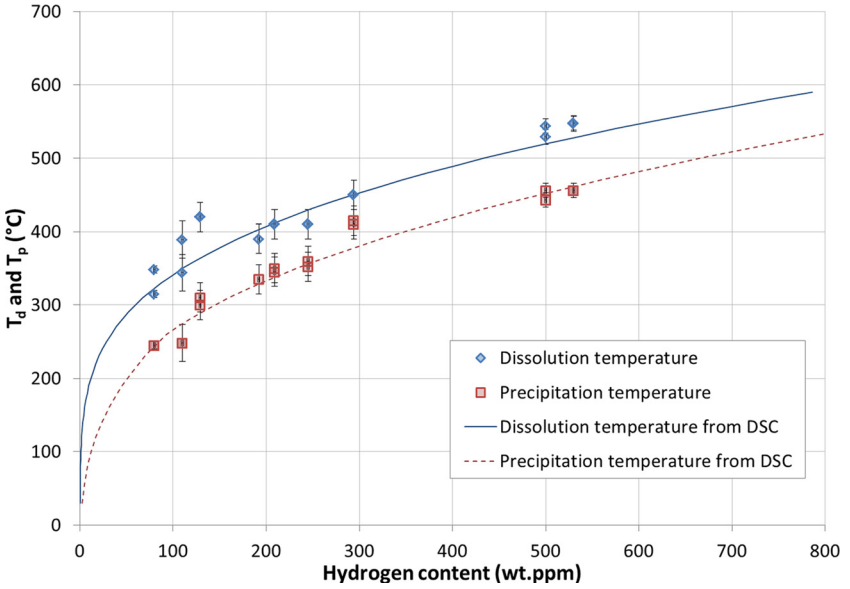

FIG. 5 Evolution of the intensity of the hydride $\delta\{111\}$ peak intensity with temperature when full dissolution is not achieved (CWSR Zircaloy-4 sample with 246 wt. ppm of hydrogen.

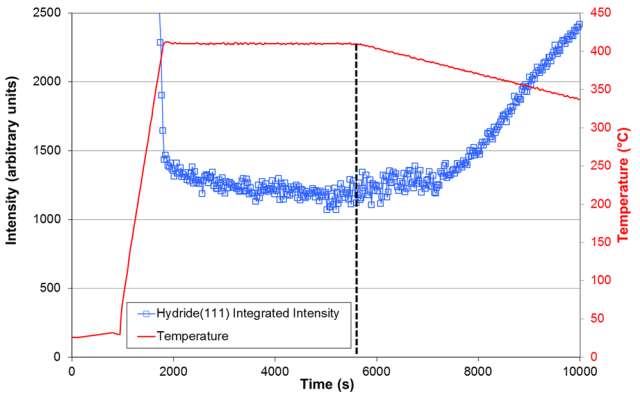

246 wt. ppm of hydrogen, which was subjected to a heat treatment at 400°C (T_d for 246 wt. ppm of hydrogen is 430°C). Because not all the hydrides dissolve in these conditions, hydrides are already present when cooldown starts. As shown in **Fig. 5**, the diffracted intensity starts to increase as soon as the temperature is decreased (without hysteresis) indicating that the hysteresis is linked to the initial hydride precipitation.

To understand the mechanisms of hydride reorientation, it is important to understand the effect of stress on hydride precipitation. Studies have shown that whereas stress does not significantly affect the solubility of hydrogen in Zircaloy, it has a strong effect on hydrogen mobility [21,22]. However, most of the studies on the effect of stress on hydride precipitation have been performed on samples in which hydride reorientation did not occur. The effect of stress and reorientation on hydride precipitation kinetics is presented in this study. The precipitation temperature was measured for samples with different hydrogen content where the hydrides were dissolved without applied stress then precipitated under different levels of applied stress (no stress, low stress below threshold stress for reorientation, and high stress above the threshold stress for reorientation). The ratio of the precipitation temperature measured in situ by XRD over that expected for unstressed material from DSC [20] is presented in **Fig. 6**. For samples precipitated under no applied stress and under low applied stress (60–160 MPa), it can be seen that the ratio is close to one which signifies the precipitation temperature remains well within the values obtained from DSC [20], and thus no significant effect of stress on T_p is observed for samples in which no hydride reorientation occurs. This is consistent with the literature results by Kammenzind et al. [21]. The error bars in **Fig. 6** were determined by the heating/cooling rate and the time between acquisitions of successive diffraction patterns similarly to those presented in **Fig. 4**. The effect of stress on the dissolution temperature is not presented here, because in most of our studies dissolution was performed under no applied stress (previous studies on the effect of stress on the dissolution temperature are presented in Ref 11). The precipitation temperature measured for samples precipitated under high applied stress (between 230 and 240 MPa), which showed some hydride reorientation are presented on the right-hand side of **Fig. 6**. It can be seen that for samples in which hydride reorientation occurs, the precipitation temperature is below the value measured from DSC. This means that a greater degree of undercooling is required to precipitate hydrides in the reoriented direction than to precipitate hydrides in their common in-plane orientation.

EFFECT OF HYDROGEN IN SOLID SOLUTION ON ZIRCONIUM STRAINS

The study of the diffraction peak positions of the hydride $\delta\{111\}$ and zirconium $\alpha\{10.0\}$ gives information on the elastic strains of these two phases during hydride dissolution and precipitation. The zirconium strain represented here is the uniaxial strain calculated using the first data point at time zero (room temperature) in the following manner:

FIG. 6 Ratio of the precipitation temperature measured in situ with XRD for several CWSR Zircaloy-4 samples with hydrogen content ranging from 80 to 530 wt. ppm precipitated under different levels of stress (no stress, low stress of 60–160 MPa and high stress between 230 and 240 MPa) over the predicted precipitation temperature without stress from DSC [20]. The threshold stress for hydride reorientation for this material is ~200 MPa.

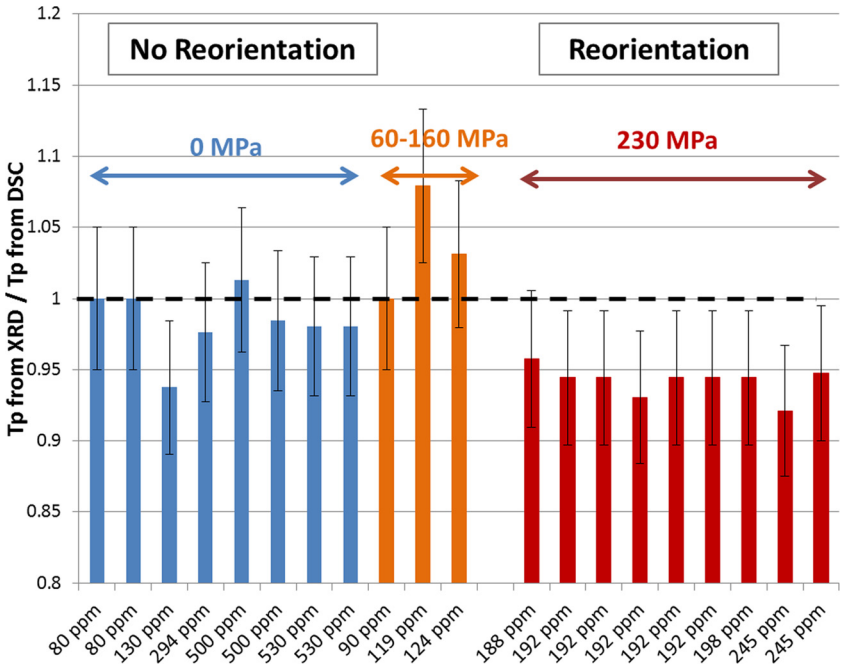

$$\varepsilon = \frac{d(\{hkl\}, T) - d(\{hkl\}, 30°\mathrm{C})}{d(\{hkl\}, 30°\mathrm{C})} \tag{1}$$

The reference *d*-spacing at room temperature for the zirconium peaks comes from the first diffraction pattern, which was recorded at room temperature (30°C) before any thermo-mechanical treatment. The formula above is only valid for the calculation of the zirconium strain; for the calculation of the hydride strain, the same formula is used but the reference *d*-spacing is no longer taken at 30°C. Further discussion on the reference *d*-spacing for the hydride strain calculation is presented in the next section.

By taking an unhydrided Zircaloy-4 sample through the temperature schedule for dissolution and precipitation and measuring the *d*-spacing increase with temperature, the coefficient of thermal expansion in the "*a*" direction for the hexagonal structure was calculated to be about $6.2 \times 10^{-6}\,°\mathrm{C}^{-1}$ in the transverse direction and

FIG. 7 Schematic of the effect of hydrogen in solid solution on zirconium strains with temperature in unhydrided and hydrided samples.

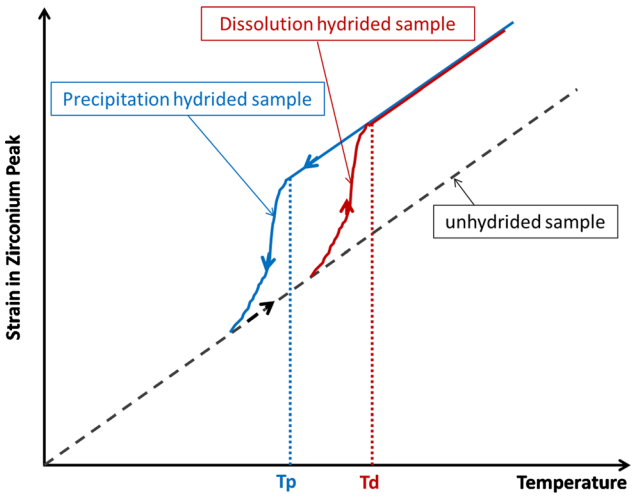

$5.6 \times 10^{-6}\,°C^{-1}$ in the rolling direction. Using the evolution of strain in the zirconium $\alpha\{00.2\}$ peak with temperature, the coefficient of thermal expansion in the "*c*" direction was found to be $8.2 \times 10^{-6}\,°C^{-1}$ in the transverse direction (there are almost no basal planes in the rolling direction, so the coefficient of thermal expansion was only calculated in the TD). These values are in close agreement with the previously reported values of the thermal expansion in the "*a*" direction, which is $5.8 \times 10^{-6}\,°C^{-1}$, and that in the "*c*" direction, which is $7.6 \times 10^{-6}\,°C^{-1}$ for CWSR Zircaloy-4 [23].

The zirconium strain behavior of hydrided samples during heating and cooling is slightly different than that of unhydrided samples. An additional contribution to the zirconium matrix strain is caused by hydrogen atoms in solid solution as the hydrides dissolve and re-precipitate. The expected effect of hydrogen atoms in solid solution on zirconium strains is schematically represented in Fig. 7. As the temperature increases from room temperature, the zirconium $\alpha\{10.0\}$ *d*-spacing increases proportionally as predicted by the thermal expansion coefficient of $6.2 \times 10^{-6}\,°C^{-1}$ in the transverse direction. When hydrides start to dissolve, the hydrogen atoms in solid solution cause an additional expansion of the zirconium planes (red, right-most curve in Fig. 7). This additional expansion ends when all hydrides are dissolved (T_d) leaving again only thermal expansion strain. During cooldown, the same process is seen in reverse as the hydrogen atoms are removed from solid solution for $T < T_p$.

Thus, the change of slope in zirconium *d*-spacing can also be used to determine the dissolution and precipitation temperatures. Figure 8 shows the measured strain

FIG. 8 Strain in TD in the zirconium α{10.0} peak in a sample with 129 wt. ppm of hydrogen heated and cooled under no applied stress. The strain in unhydrided material is represented as well.

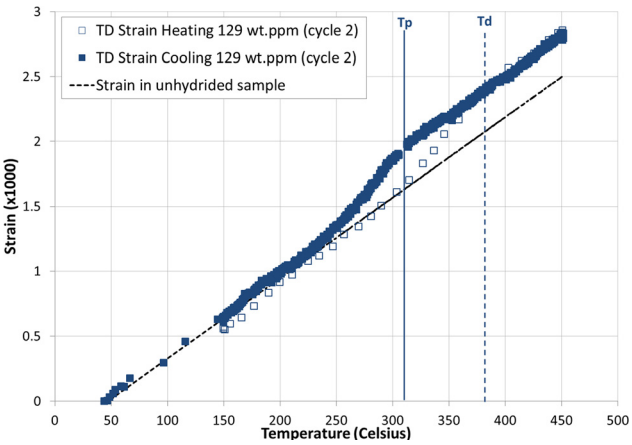

in the TD for the zirconium α{10.0} peak in a sample with 129 wt. ppm of hydrogen. As the temperature increases, the strain initially follows the expected thermal expansion behavior. At around 250°C, significant hydride dissolution starts to occur. This process accelerates, until above 380°C (T_d) the strain again follows the thermal expansion curve (all hydrogen in solid solution). Upon cooling, a change of slope of the zirconium strain occurs at about the hydride precipitation temperature, as hydrides start precipitating and fewer atoms remain in solid solution in the matrix, which reduces strain. Once most hydrides have precipitated, the zirconium strain becomes again governed by thermal expansion only. The deviation from the ideal *d*-spacing is more pronounced for samples with higher hydrogen content, as can be seen in Fig. 9 where zirconium strains in a sample containing 294 wt. ppm of hydrogen are shown. These effects of hydrogen on zirconium strains are coherent with the schematic representation of Fig. 7.

The hydride phase elastic strains during hydride dissolution and precipitation can also be studied by a manner similar as in the zirconium phase as presented in the following paragraphs.

HYDRIDE STRAINS DURING NUCLEATION AND GROWTH

Thermo-Mechanical Cycle Without Applied Stress.

The elastic strain in the hydride as measured using the δ{111} planes in the TD in a sample with 294 wt. ppm of hydrogen are presented in Fig. 10 as the hydrides are dissolved and re-precipitated. As the temperature increases, the hydrides dissolve and the hydride *d*-spacing follows the same trend as the zirconium *d*-spacing (as

FIG. 9 Strain in TD in the zirconium $\alpha\{10.0\}$ peak in a sample with 294 wt. ppm of hydrogen heated and cooled under no applied stress.

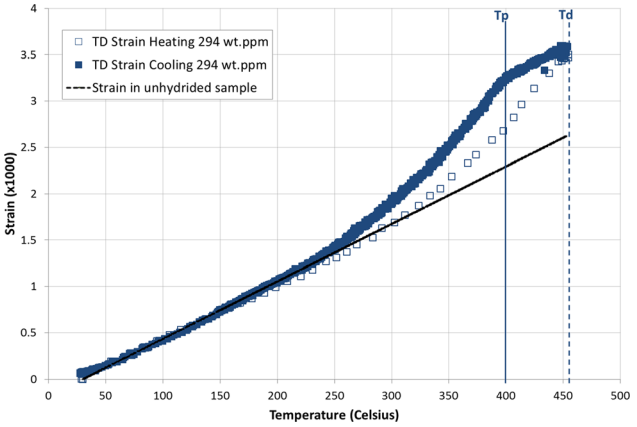

seen in Fig. 9), rather than the thermal expansion coefficient of hydrides of $14.2 \times 10^{-6}\,°C^{-1}$ [23], likely because their expansion is limited by being embedded in the matrix. In the final stages of dissolution, the hydrogen in solid solution increases the zirconium *d*-spacing (as discussed in the previous paragraph), whereas the hydride *d*-spacing is very close to the unstressed *d*-spacing value from the

FIG. 10 Hydride strain behavior during cooling (calculated from $\delta\{111\}$ peaks in the TD) in a sample with 294 wt. ppm of hydrogen cooled without applied stress. Specific locations noted that A, B, C, D, and E correspond to the schematic in Fig. 17.

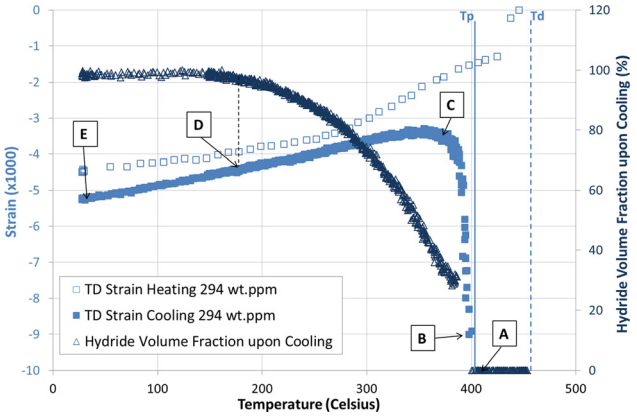

FIG. 11 Strain in RD in the hydride $\delta\{111\}$ peak in a sample with 294 wt. ppm of hydrogen heated and cooled under no applied stress.

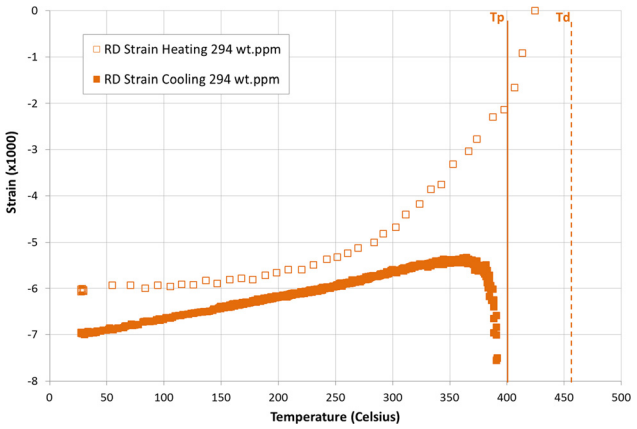

literature [24] calculated at $T = 450°C$, of 2.7672 Å. This value of the d-spacing was found at the final stage of dissolution, approximately, for most samples, and therefore this final d-spacing value was taken as the reference value for unstressed hydride lattice parameter.

Beyond 450°C, all diffraction signals disappear, so the hydrides are completely dissolved (point A). As the temperature is decreased, precipitation starts to occur when the temperature falls below the precipitation temperature of 398°C (point B). At that stage, a small diffraction peak appears. Analysis of the peak full-width at half-maximum (see section on Hydride Peak Broadening below) shows that down to 354°C, size broadening is the dominant mechanism. The other feature is that the $\delta\{111\}$ d-spacing in the TD (**Fig. 10**) and in the RD (**Fig. 11**) is much lower than the unstressed value, likely indicating that these particles are under compression at about 10 millistrains, which corresponds to a stress of 660 MPa at their edges.[6] The average compressive strain of the hydride population decreases as the temperature decreases to 375°C (point C). This could be because of a change of shape from sphere to plate as the precipitate grows. In the case of platelet-shaped precipitates, shear stresses can lead to formation of dislocations in the matrix (whereas for spheres, only hydrostatic stresses are present, thus creating no shear stresses that generate dislocations). It is also possible that "sympathetic nucleation," by which a new hydride nucleus precipitates within the strain field of neighboring hydrides

[6] It is also possible that this high compressive strain, which is a diffraction peak shift, could be because of the initially forming hydrides having a slightly different stoichiometry than the Zr/H ratio of 1.66 typical in the δ-hydride phase. Within the δ-hydride phase, a maximum change in d-spacing because of stoichiometry of 0.002 nm could lead to a pseudo-strain of 4 millistrain [26,27].

(thus requiring less strain to form), contributes to the decrease in average strain of the hydride population during precipitate growth in cooldown. The available data does not enable us to distinguish between these possible causes. In addition, the phenomenon of high stress zirconium creep could induce local relaxation of the hydride strains. However, the zirconium diffraction data is averaged over many grains, a majority of which do not contain hydrides. Therefore, local effects on the zirconium phase cannot be measured with this technique.

One might consider that the higher differential thermal expansion of hydrides ($14.2 \times 10^{-6}\,°C^{-1}$) compared to that of zirconium ($6 \times 10^{-6}\,°C^{-1}$) [23] could cause some relaxation upon cooldown as the hydride shrinks away from the matrix. A simple calculation indicates that it would only account for 7 %–10 % of the strain relaxation observed from 400°C to 375°C [on a temperature change of 50°C, $\varepsilon_{\text{thermal difference}} = 50 \times (14.2 \times 10^{-6} - 6 \times 10^{-6}) = 0.4$ millistrain]. At 375°C, half of the hydrides have precipitated and the strains start to follow the thermal expansion of zirconium, i.e., decreasing with decreasing temperature (from point C to points D and E). This suggests that below this temperature less nucleation occurs and additional hydrogen precipitation occurs by growth of existing hydrides. As a consequence, less relaxation is observed associated with a post-nucleation change of shape and/or dislocation formation. The strain value at room temperature after the thermal cycle suggests that hydrides are subjected to a compressive stress of about ~500–700 MPa, which is below the hydride yield stress of about 800 MPa [26–28] (calculated using a multi-axial stress state) [18]. The observed strain behavior is the same in the rolling direction as in the transverse direction as can be seen in Fig. 11. This is logical because, in both cases, the planes observed are the side {111} planes of the hydride platelet, and the texture and microstructure of the edges or the hydrides are expected to be similar in the TD and the RD.

THERMO-MECHANICAL CYCLE WITH 160 MPA APPLIED STRESS: NO HYDRIDE REORIENTATION

In the sample studied here, a stress of 160 MPa was applied, which was not sufficient to induce any reorientation of hydrides as seen in Fig. 3. This allows us to investigate the effects of stress in circumferential hydrides and reoriented hydrides. Figure 12 shows the strains in the zirconium matrix, calculated using the zirconium α{10.0} peaks, as a function of temperature in the TD and the RD. The 160 MPa stress was applied in the TD during cooling. The tensile frame was operated in load control, ensuring that a constant load was applied on the sample during cooling. As the temperature increases, the *d*-spacing increases because of thermal expansion. When hydrogen starts to dissolve into the matrix in significant quantities, the strain deviates from thermal expansion as shown in Fig. 12. The change of slope of the zirconium matrix strain as hydrides dissolve and re-precipitate is similar to that observed in Fig. 8. The load was applied at high temperature and removed at 150°C as shown in Fig. 12. The applied load stretches the zirconium α{10.0} planes in the

FIG. 12 Strain in the zirconium α{10.0} peak in a sample with 124 wt. ppm of hydrogen heated and cooled under 160 MPa tensile stress: (*a*) in the TD; and (*b*) in the RD.

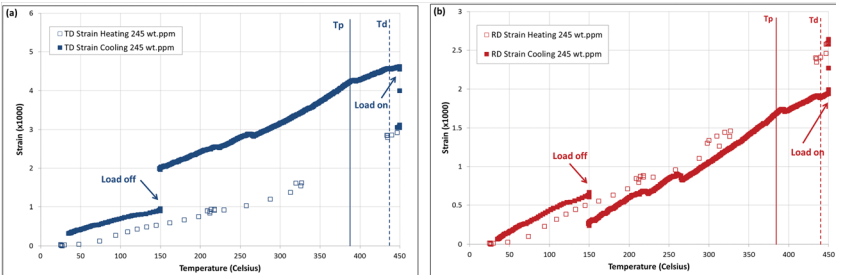

TD and compresses them in the RD by Poisson's effect, as seen in Fig. 12.[7] When the load is removed, the value of the Zr{10.0} *d*-spacing in the RD returns to its expected *d*-spacing value; however, the TD planes remain a little stretched by approximately 0.2 millistrain compared to the unstressed value in Fig. 8. This could be because of relaxation of the residual compressive strains of the zirconium matrix caused by manufacturing of the material (the effect is mitigated in the RD because of a Poisson's ratio of 0.32 [28]).

Figure 13 shows the elastic strains in the δ{111} hydride peaks measured in the TD and the RD for a sample with 245 wt. ppm of hydrogen when cooled under

FIG. 13 Strain in the hydride δ{111} peak in a sample with 245 wt. ppm of hydrogen heated and cooled under 160 MPa tensile stress: (*a*) in the TD; and (*b*) in the RD.

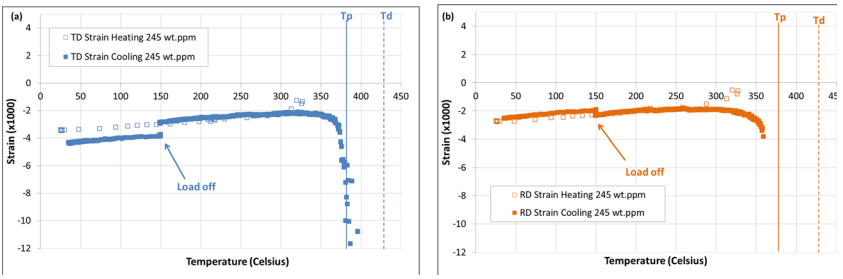

[7] When a tensile stress is applied in the TD, Poisson's ratio is defined as $\nu = -d\varepsilon(\mathrm{ND})/d\varepsilon(\mathrm{TD}) = -d\varepsilon(\mathrm{RD})/d\varepsilon(\mathrm{TD})$. For small deformations, $\nu \approx \Delta d(\mathrm{RD})/\Delta d(\mathrm{TD}) = \Delta d(\mathrm{ND})/\Delta d(\mathrm{TD})$ [3].

160 MPa applied tensile stress. The evolution of hydride strains during hydride dissolution shown in Figs. 13(*a*) and 13(*b*) is similar to that observed in Fig. 10. This is logical because hydrides were dissolved under no applied stress. During cooling, the first regime of precipitation is similar to that of unstressed samples and starts at about the same compressive strain of 10 millistrain as seen in Fig. 13(*a*). Even when formed under stress, hydride particles start as highly compressed small precipitates, then relax some of these compressive strains as they grow, change shape, and form dislocations as discussed above. The change to the second regime of precipitation occurs at 350°C, which is also when half of the hydrides are precipitated as can be determined by the hydride volume fraction curve obtained from the hydride peak intensity curve similarly to that obtained in Fig. 10, but not shown here for the sake of clarity. In the case of the 294 wt. ppm sample, the change of precipitation regime also occurred at a temperature when half of the hydride population was precipitated. However, the hydride strains observed in this secondary regime at lower temperatures are different from those observed in the unstressed sample. In the stressed sample, hydride compressive strains depend less on temperature and are more constant, even though the entire system is cooling. This could be explained by the fact that under a far-field strain, the zirconium matrix deforms more easily and transfers some of the tensile strain to the hydride. This load transfer gives enough tensile stress to compensate for the compressive strains that would otherwise appear because of cooling. This explanation has been advanced by Kerr et al. when they studied room temperature deformation of hydrided samples [14]. Finally, this explanation is also in agreement with the fact that when the applied load is removed at 150°C, the hydrides planes in the RD are slightly less compressed (and those in the TD are slightly more compressed) than initially at that temperature (seen from the dissolution curve), which would indicate that some strain relaxation occurs in hydrides grown under tensile stress.

THERMO-MECHANICAL CYCLE WITH 240 MPA APPLIED STRESS: HYDRIDE REORIENTATION

In this section, we discuss a sample that has been cooled under an applied stress of 240 MPa, thus leading to hydride reorientation, as seen in Fig. 3. Figure 14 shows the strain in the hydride $\delta\{111\}$ peak for the planes oriented along the transverse and the rolling directions. During heating (performed under no applied stress), the strain curves in the TD and the RD are similar to those observed for unstressed samples as would be expected. As shown in Fig. 14(*a*), when the temperature reaches 330°C during cooling, the hydrides initially precipitate in a highly compressed state. As the temperature decreases further, the magnitude of the strain in the TD decreases and then actually becomes *positive*. The hydride strain in the RD, shown in Fig. 14(*b*), are also seen to be compressive at the onset of hydride precipitation, and the compressive strain decreases as the temperature decreases, remaining however in the compressive regime throughout. Once the secondary regime kicks in,

FIG. 14 Strain of the hydride {111} peak in a sample with 192 wt. ppm of hydrogen cooled under a 240 MPa applied stress applied in the TD, reorientation of hydrides: (*a*) in the TD; and (*b*) the RD.

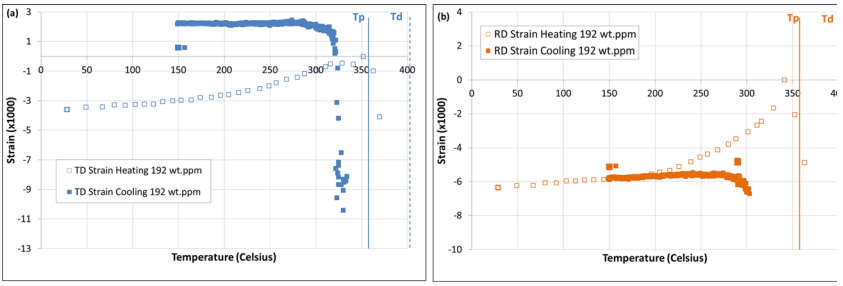

the strains remain approximately constant, except one is tensile and the other compressive.

The measured hydride tensile strains in the TD could be because of the fact that we are now observing reoriented hydride planes on the *face* of the hydride platelet and no longer on the edge, as for circumferential hydrides and due to the applied tensile stress in the TD, those reoriented hydride faces could be in tension. The measured hydride compressive strains in the RD could be caused by the compressive stress applied by the matrix because of the applied tensile stress in the TD (compression by Poisson's effect), or because the hydride planes in the RD are the *edges* of the reoriented hydride platelets, in contrast to those planes observed in the TD.

HYDRIDE PEAK BROADENING

The third parameter analyzed by the fitting of the diffraction peaks is the peak width or full-width at half-maximum (FWHM). The broadening of these x-ray diffraction peaks can be caused by several factors including instrumental broadening. The instrumental broadening was measured using a powder standard and removed by quadratic subtraction $[\mathrm{FWHM}_{\mathrm{sample}} = \sqrt{(\mathrm{FWHM}_{\mathrm{measured}}{}^2 - \mathrm{FWHM}_{\mathrm{instrumental}}{}^2)}]$. Once instrumental broadening has been removed, both strain broadening and size broadening need to be considered. To quantitatively differentiate between strain and size broadening and to better understand the general state of strain of the hydrides, an analysis was carried out using Williamson–Hall plots [29]. The following relations allow us to distinguish between the two types of broadening:

$$\mathrm{FWHM}_{\mathrm{sample}} \propto \varepsilon_{\mathrm{lattice}} \frac{\sin\theta}{\cos\theta} \quad \text{strain broadening} \tag{2}$$

$$\mathrm{FWHM}_{\mathrm{sample}} \propto \frac{0.9\lambda}{t\cos\theta} = \delta \quad \text{size broadening} \tag{3}$$

FIG. 15 Schematic representation of a Williamson-Hall plot.

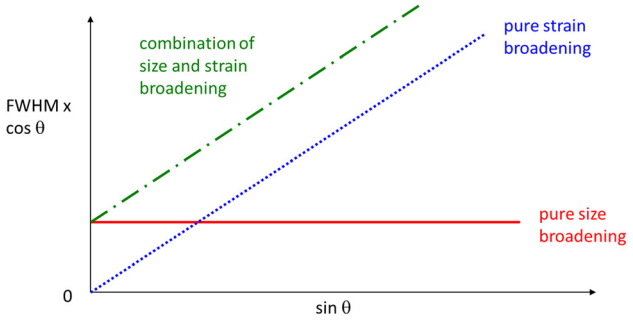

where $FWHM_{sample}$ is the measured Gaussian FWHM minus the instrumental broadening (in radians 2θ), θ is the Bragg angle (in radians), $\varepsilon_{lattice}$ is the root-mean-square strain, t is the sample particle size (in nm), and λ is the x-ray beam wavelength (in nm). A Williamson–Hall plot presents FWHM $\times \cos\theta$- noted B- as a function of $\sin\theta$ for different peaks of the same phase as represented schematically in Fig. 15. Strain broadening varies with the 2θ value of the peak under consideration, whereas size broadening is independent of angle when plotted in the Williamson-Hall plots. Therefore, in a Williamson-Hall plot, the slope of the curves plotted is proportional to strain, and the y-intercept is proportional to the amount of size broadening.

This plot was done for the δ-hydride phase using the {111} and {220} peaks during cooling, the slopes and y-intercept were then obtained for the sample with 294 wt. ppm of hydrogen heated and cooled under no applied stress. The evolution of the slope and intercept of these Williamson-Hall curves (WH) can then be followed as a function of temperature as the hydrides are dissolved and re-precipitated. The results for these fits are presented in Fig. 16. Fits of higher

FIG. 16 (*a*) Slope, and (*b*) intercept of the Williamson-Hall plots for a sample with 294 wt. ppm of hydrogen, heated and cooled under no applied stress.

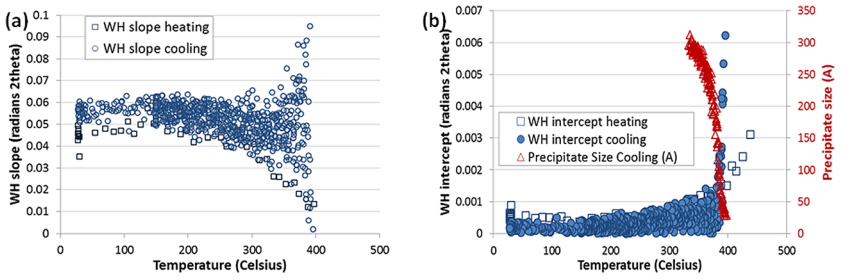

temperature diffraction patterns are, of course, less accurate than those obtained at lower temperatures because, at the onset of hydride precipitation, hydride diffraction peaks are quite small and thus difficult to fit with confidence. The scatter observed in the determination of the slope is caused in part by the difficulty of fitting small diffraction peaks. In addition, the WH fits in this figure are based on the only two hydride diffraction peaks available, and thus would add another level of uncertainty and increase scatter in the WH data. However, the overall trends of the change of slope with temperature can be discerned in these WH plots.

Indeed, it can be seen in **Fig. 16** that the slope of the WH plot decreases as the temperature increases, approaching zero at the dissolution temperature. This is logical as the strain should decrease as the particle size becomes smaller. In contrast the *y*-intercept is small initially, increasing as the particle dissolves. This suggests that above 375°C, there is mostly size broadening in our samples, whereas below 375°C, the peak broadening is dominated by strain. In **Fig. 16(*b*)**, the size of the particles as calculated using Eq 3 is shown. It should be noted that after 325°C, only strain broadening is detected, so the particle size may be changing without being detected by the size-broadening technique. The initial diameter of the particles forming at high temperatures, calculated using Eq 3, is about 25 Å. When the particle size reaches approximately 300 Å, the size-broadening effect becomes negligible compared to the strain-broadening effect.

Discussion

Two different aspects of hydride and matrix strains have been presented in the previous sections: (i) the evolution of elastic strains calculated from the shift in peak positions, and (ii) the evolution of the FWHM of these diffraction peaks with temperature. The first yields information on the average elastic strains in the diffracting phase, and the second on non-uniform elastic strain and the distribution of elastic strain in the sampled volume as well as information on the size of the diffraction particles.

In samples cooled without applied stress, at any given temperature above the solubility limit, the hydrogen in solid solution causes the zirconium lattice parameter to be higher than that of zirconium without hydrogen in solid solution. The precipitation temperature then corresponds to the temperature at which the lattice parameter variation with temperature changes slope. This allowed us to verify that the precipitation temperature matched well with the precipitation temperature values obtained from DSC.

A simplified view of the precipitation mechanism can be considered as follows. Hydride particles form as highly compressed, small precipitates as seen in **Fig. 17(*a*)** (the hydride nuclei are represented in dark red because of their high compressive strain state). The small precipitate size is estimated from the size broadening observed in the diffraction signal, whereas the compressive strain state is estimated by the shift in hydride peak position. As the temperature decreases, the hydride

FIG. 17 Schematic of hydride strain behavior during cooling without applied stress: (*a*) all hydrides are dissolved, (*b*) first hydride nuclei appear, (*c*) previous hydride nuclei grown and relaxed (dislocations in the matrix), new hydride nuclei form less compressed (sympathetic nucleation), (*d*) all hydrides are precipitated, and (*e*) precipitated hydrides in compression because of thermal contraction.

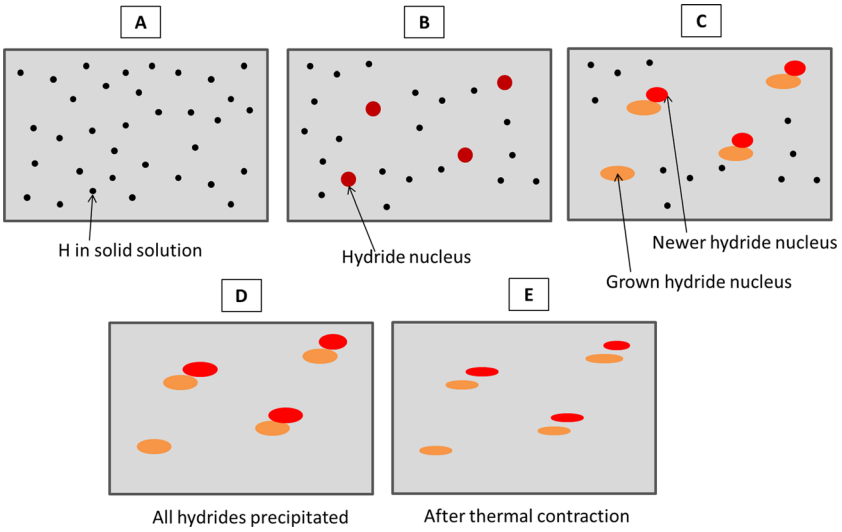

volume fraction increases as a result of nucleation of new precipitates and growth of the previous ones. The average strain increases (Fig. 17(*b*)) indicating that the new hydride precipitates are less compressed or that some strain is relaxed by plastic deformation. This continues until the hydride strain reaches $\sim -3.5 \times 10^{-3}$ at which point half of the hydride population is precipitated (Fig. 17(*c*)). From this point down to room temperature, hydride strains follow the thermal contraction of the zirconium matrix (thermal expansion coefficient of $6.2 \times 10^{-6} \,^{\circ}\mathrm{C}^{-1}$) instead of the hydride thermal contraction (thermal expansion coefficient of $14.2 \times 10^{-6} \,^{\circ}\mathrm{C}^{-1}$). Although the hydrides would like to contract further away from the matrix, they are forced to follow thermal contraction of the matrix likely because the hydride particles are embedded in the matrix (Fig. 17(*d*) and 17(*e*)). From 450°C to 360°C, the hydride $\delta\{111\}$ diffraction peaks show predominantly size broadening and the hydride size grows from 2.5 to 30 nm. From 360°C to room temperature, the dominant broadening mechanism is strain broadening. This strain broadening is constant, showing that the strain distribution in the hydride population is constant from 360°C to room temperature.

A similar behavior is observed in samples cooled under an applied stress below the critical value to reorient hydrides. The zirconium matrix deforms slightly because of the thermal cycle under applied stress. Hydride precipitation occurs at

the expected precipitation temperature for unstressed hydrides. Hydride precipitation is also divided into two precipitation regimes. The first precipitation regime occurring at high temperature is nearly identical to that of unstressed hydrides. The onset of the second precipitation regime also occurs when half of the hydride population is precipitated. Hydride strains during this second precipitation regime evolve differently than in unstressed hydrides. The strains in the case of stressed hydrides remain constant as the hydrides finish precipitating and cool down to room temperature. This is likely because of the fact that in the presence of the far field strain, the matrix deforms more easily and transfers load to the hydrides, thus compensating for thermal contraction. Hydrides are still in compression after the load is removed in both TD and RD although slightly less in the TD where the tensile load had been previously applied.

In samples cooled under an applied stress sufficient for reorientation, hydride precipitation occurs at a temperature below the value obtained from DSC under no load. During the first precipitation regime, the measured hydrides strains are compressive, but as the temperature decreases these strains become tensile in the direction of the applied stress (TD). During the second precipitation regime, hydride strains in the direction of the load remain constant and tensile. These strains remain tensile (although less) even after the load is removed. Hydride strains are compressive in the direction perpendicular to the load (RD) during cooldown. These strains also become compressive once the load is removed.

Conclusions

The main conclusions of the study of hydrides in uniformly stressed samples in cold-worked stress-relieved Zircaloy-4 are presented here:

1. The hydride dissolution and precipitation temperatures were determined in situ by synchrotron XRD, and validated by comparison to previous DSC determination finding good agreement in that the hysteresis observed between dissolution and precipitation temperatures corresponds to values measured previously by DSC in the absence of stress. This means that the dissolution and precipitation temperatures can be directly determined from each sample examination.
2. For a stress *above* the threshold stress for reorientation, it is found that the precipitation temperature is *lower* than that of unstressed samples. For a stress *below* the threshold stress for reorientation, the precipitation temperature corresponds to the unstressed value.
3. The change in hydride *d*-spacing was measured during hydride dissolution and precipitation by transmission XRD. Considering that most of the *d*-spacing change is because of strain, when unstressed hydrides precipitate, two strain regimes are observed. Hydrides first nucleate as highly compressed particles, then quickly relax some of these compressive strains by either change of shape, sympathetic nucleation, or formation of dislocations in the matrix. When half of the hydride population is precipitated, the hydride strain

behavior changes to follow the matrix thermal expansion all the way down to room temperature.

4. When hydrides are precipitated under stress but not reoriented, the strain behavior is different than that of unstressed hydrides. The first precipitation regime with relaxation of highly compressed particles is similar to that of unstressed hydrides. However, the average hydride strain during the second precipitation regime is constant. This could be because of a greater ease in deforming the matrix because of the applied far-field stress.
5. When hydrides precipitate under stress and reorient, during the first precipitation regime, the hydride strains become tensile in the direction perpendicular to the hydride platelet face. During the second precipitation regime, these strains remain constant in tension. This indicates a different hydride strain state for reoriented hydrides than for circumferential hydrides. Neither cycling under stress nor increasing cooling rate appear to significantly affect the strain state of reoriented hydrides.

ACKNOWLEDGMENTS

This research is funded by the Materials World Network grant DMR-0710616 from the National Science Foundation, with corresponding funding from NSERC for the Canadian partners. The writers are grateful for their support. The research for this publication was supported by the Pennsylvania State University Materials Research Institute Nano Fabrication Network and the National Science Foundation Cooperative Agreement No. 0335765, National Nanotechnology Infrastructure Network with Cornell University. Use of the Advanced Photon Source is supported by the U.S. Department of Energy, Office of Basic Energy Sciences under Contract No. DE-AC02-06CH11357.

References

[1] Lemaignan, C. and Motta, A. T., "Zirconium Alloys in Nuclear Applications," *Materials Science and Technology, A Comprehensive Treatment*, R. W. Cahn, P. Haasen, and E. J. Kramer, Eds., VCH, New York, 1994, pp. 1–51.

[2] Bossis, P., Pêcheur, D., Hanifi, L., Thomazet, J., and Blat, M., "Comparison of the High Burn-up Corrosion on M5 and Low Tin Zircaloy-4," *Zirconium in the Nuclear Industry: 14th International Symposium, ASTM STP 1467*, P. Rudling and B. F. Kammenzind, Eds., 2005, pp. 494–525.

[3] Schmitz, F. and Papin, J., "High Burnup Effects on Fuel Behaviour Under Accident Conditions: The Tests CABRI REP-Na," *J. Nucl. Mater.*, Vol. 270, 1999, pp. 55–64.

[4] Daum, R. S., 2007, "Hydride-Induced Embrittlement of Zircaloy-4 Cladding under Plane-Strain Tension," Ph.D. thesis, Materials Science, The Pennsylvania State University, University Park, PA.

[5] Raynaud, P. A. C., Koss, D. A., and Motta, A. T., "Crack Growth in the through-Thickness Direction of Hydrided Thin-Wall Zircaloy Sheet," *J. Nucl. Mater.*, Vol. 420, 2012, pp. 69–82.

[6] Bradbrook, J. S., Lorimer, G. W., and Ridley, N., "The Precipitation of Zirconium Hydride in Zirconium and Zircaloy-2," *J. Nucl. Mater.*, Vol. 42, No. 2, 1972, pp. 142–160.

[7] Beck, R. L., "Zirconium-Hydrogen Phase System," *Trans. ASM*, Vol. 55, 1962, pp. 542–555.

[8] Chung, H. M., Daum, R. S., Hiller, J. M., and Billone, M. C., "Characteristics of Hydride Precipitation in Spent-Fuel Cladding," *Zirconium in the Nuclear Industry: 13th International Symposium, ASTM STP 918*, 2002, pp. 78–101.

[9] Kearns, J. J. and Woods, C. R., "Effect of Texture, Grain Size, and Cold Work on the Precipitation of Oriented Hydrides in Zircaloy Tubing and Plate," *J. Nucl. Mater.*, Vol. 20, No. 3, 1966, pp. 241–261.

[10] Fredette, J. C., Perovic, V., and Holt. R. A., "Orientation of Hydrides in Zr-2.5Nb Tubes Under Biaxial Stress," *Zirconium in the Nuclear Industry: 15th International Symposium, ASTM STP 1505*, B. F. Kammenzind and M. Limback, Eds., June 25–28, Sunriver, OR, 2007.

[11] Colas, K. B., Motta, A. T., Almer, J. D., Daymond, M. R., Kerr, M., Banchik, A. D., Vizcaino, P., and Santisteban, J. R., "In-Situ Study of Hydride Precipitation Kinetics and Re-Orientation in Zircaloy Using Synchrotron Radiation," *Acta Mater.*, Vol. 58, 2010, pp. 6565–6583.

[12] Zanellato, O., Preuss, M., Buffiere, J.-Y., Ribeiro, F., Steuwer, A., Desquines, J., Andrieux, J., and Krebs, B., "Synchrotron Diffraction Study of Dissolution and Precipitation Kinetics of Hydrides in Zircaloy-4," *J. Nucl. Mater.*, Vol. 420, 2012, pp. 537–547.

[13] Kerr, M., 2009, "Mechanical Characterization of Zirconium Hydrides With High Energy X-Ray Diffraction," Ph.D. thesis, Mechanical and Materials Engineering, Queen's University, Kingston, ON, Canada.

[14] Kerr, M., Daymond, M. R., Holt, R. A., and Almer, J. D., "Strain Evolution of Zirconium Hydride Embedded in a Zircaloy-2 Matrix," *J. Nucl. Mater.*, Vol. 380, Nos. 2–3, 2008, pp. 70–75.

[15] Link, T. M., Koss, D. A., and Motta, A. T., "Failure of Zircaloy Cladding under Transverse Plane-Strain Deformation," *Nucl. Eng. Design*, Vol. 3, 1998, pp. 379–394.

[16] Perovic, V., Weatherly, G. C., and Simpson, C. J., "Hydride Precipitation in α/β Zirconium Alloys," *Acta Metall.*, Vol. 31, No. 9, 1983, pp. 1381–1391.

[17] Daum, R. S., Majumdar, S., Liu, Y., and Billone, M. C., "Mechanical Testing of High-Burnup Zircaloy-4 Fuel Cladding under Conditions Relevant to Drying Operations and Dry-Cask Storage," *Water Reactor Fuel Performance Meeting*, Oct 3–6, Kyoto, Japan, 2005, pp. 498–531.

[18] Colas, K. B., Motta, A. T., Daymond, M. R., Kerr, M., and Almer, J. D., "Hydride Platelet Reorientation in Zircaloy Studied With Synchrotron Radiation Diffraction," *J. ASTM Int.*, Vol. 88, No. 1, 2011.

[19] Larson, A. C. and Dreele, R. B. V., *General Structure Analysis System (GSAS)*, Los Alamos National Laboratory, Los Alamos, NM, 2000.

[20] Une, K. and Ishimoto, S., "Dissolution and Precipitation Behavior of Hydrides in Zircaloy-2 and High Fe Zircaloy," *J. Nucl. Mater.*, Vol. 322, No. 1, 2003, pp. 66–72.

[21] Kammenzind, B. F., Berquist, B. M., Bajaj, R., Kreyns, P. H., and Franklin, D. G., "The Long-Range Migration of Hydrogen through Zircaloy in Response to Tensile and Compressive Stress Gradients," *Zirconium in the Nuclear Industry: 12th International Symposium, ASTM STP 1354*, G. P. Sabol and G. D. Moans, Eds., June 15–18, 2000, pp. 196–233.

[22] Eadie, R. L. and Coleman, C. E., "Effect of Stress on Hydride Precipitation in Zirconium-2.5% Niobium and on Delayed Hydride Cracking," *Scripta Metall.*, Vol. 23, No. 11, 1989, pp. 1865–1870.

[23] Douglass, D. L., "The Metallurgy of Zirconium," *Atomic Energy Review*, Z. I. Turkov, Ed., International Atomic Energy Agency, Vienna, Austria, 1971.

[24] *The Powder Diffraction File*, International Center for Diffraction Data, Newtown Square, PA, 2006.

[25] Zuzek, E., Abriata, J. P., San-Martin, A., and Manchester, F. D., "The H-Zr (Hydrogen-Zirconium) System," *Bull. of Alloy Phase Diag.*, Vol. 11, No. 4, 1990, pp. 385–395.

[26] Yamanaka, S., Yamada, K., Kurosaki, K., Uno, M., Takeda, K., Anada, H., Matsuda, T., and Kobayashi, S., "Characteristics of Zirconium Hydride and Deuteride," *J. Alloys Compd.*, Vols. 330–332, 2002, pp. 99–104.

[27] Puls, M. P., Shi, S.-Q., and Rabier, J., "Experimental Studies of Mechanical Properties of Solid Zirconium Hydrides," *J. Nucl. Mater.*, Vol. 336, No. 1, 2005, pp. 73–80.

[28] Yamanaka, S., Yoshioka, K., Uno, M., Katsura, M., Anada, H., Matsuda, T., and Kobayashi, S., "Thermal and Mechanical Properties of Zirconium Hydride," *J. Alloys Compd.*, Vols. 293–295, 1999, pp. 23–29.

[29] Snyder, R. L., Fiala, J., and Bunge, H., "Defect and Microstructure Analysis by Diffraction," *International Union of Crystallography Monographs on Crystallography*, Oxford University Press, New York, 1999.

[30] Cook, C. S., Sabol, G. P., Sekera, K. R., and Randall, S. N., "Texture Control in Zircaloy Tubing Through Processing," *Zirconium in the Nuclear Industry: 9th International Symposium, ASTM STP 1132*, Nov. 5–8, Kobe, Japan, ASTM International, West Conshohocken, PA, 1991, pp 80–95.

DISCUSSION

Question from Ron Adamson, Zircology Plus

Q1:—Do I interpret one of your curves to indicate that lattice strain caused by H in solution is different than lattice strain caused by hydride? This is different than commonly assumed and indicated by the modeling work of Wolf et al. in this meeting.

Authors' Response:—Hydrides generate both elastic and plastic strain while hydrogen in solid solution generates only elastic strain. The strain measured here is only elastic strain. The hydrides will have a small volume fraction around them where the elastic strain field is present, but this is a relatively small overall volume fraction of the whole material. The difference observed in the effect of hydrogen in hydrides and in solid solution on zirconium matrix elastic strains is due to the fact that the X-ray beam probes a large number of zirconium grains. Indeed, the in-situ synchrotron diffraction technique used in this work has a beam size of 200 μm x 200 μm and the beam goes through the entire sample thickness which is around 600 μm. Therefore for our CWSR material, hundreds of zirconium grains are sampled. When hydrogen is precipitated in hydrides, the strain induced by the hydrides on the zirconium lattice is localized around the hydrides themselves, therefore the diffraction signal from the zirconium comes from many grains without hydrides and a few with hydrides, thus the strains due to the hydrides is not measured when all hydrogen is precipitated. When all hydrogen comes into solid solution it induces a uniform strain in all the zirconium grains measured thus it is visible in the diffraction signal.

We note that when the temperature increases the lattice parameter change is occurring as the hydrides are dissolving, so the increase in lattice parameter is properly attributed to hydrogen in solid solution.

Q2:—Are you convinced that you were observing δ (delta) hydride?

Authors' Response:—When observing the diffraction patterns at room temperature (an example of which can be found in [1]), the position of the hydride peaks are consistent with those expected from δ-hydrides (Powder Diffraction File number 00-034-0649). At very high temperature when the hydrides first form, it is possible that there could be some change in stoichiometry that could induce a peak shift (see 'Thermo-mechanical cycle without applied stress' section in the paper).

Questions from K. Kapoor, NFC

Q1:—Does the hydride orientation have a memory effect?

Authors' Response:—Given the fact that when several thermo-mechanical cycles are applied, the radial hydride fraction increases, it does appear that there is a hydride orientation memory effect. This effect is essentially the same as the hydride memory effect observed for circumferential hydrides and is normally ascribed to dislocations "nests" created during the nucleation of the original hydrides and in which hydrides can re-form and grow. If the maximum temperature of the thermo-mechanical cycle is not high enough to recover the material, the hydrides will likely tend to preferentially re-precipitate in these nests.

Q2:—Why do you need multiple cycles to reorient all of the hydrides?

Authors' Response:—The need to cycle a sample several times to reach a fully reoriented microstructure could be due to the fact that our cooling rate of 1 °C/min is too fast to allow all hydrides to nucleate in the preferred out of plane orientation. Several cycles will allow a greater percentage of hydrides to form in the preferred direction. This cooling rate was a compromise chosen to be able to perform experiments in-situ at the APS synchrotron that would finish in a reasonable time.

Q3:—Why did you select (111) δ hydride peak for strain measurement?

Authors' Response:—The (111) δ hydride peak is the most intense hydride peak that can be measured with our experimental geometry and can thus give the greatest accuracy in its determination.

Question from Johannes Bertsch, Paul Scherer Institute:—Have you kept the load until the complete cool down, so that the reorientated hydrides remained under the influence of external stress? If yes, what would the stress of the hydrides be after unloading?

Authors' Response:—As can be seen in Figure 3(b) and 3(c) which represent typical thermo-mechanical cycles performed at the APS, the applied tensile load is kept constant until 150 °C at which temperature all hydrides are precipitated. Diffraction data are still acquired after the load is removed and can be seen in Figure 13 after the 'Load off' step for the stressed but not reoriented sample and in Figure 14 after the strain step at 150 °C for the reoriented sample. As can be seen from these figures, when the applied stress is removed, the hydride strains in the TD and the RD for the non-reoriented sample remain both compressive. However, the hydride strains in the TD for the reoriented samples remains positive even though the applied tensile load is removed, implying the reoriented hydride faces are in tension even without applied stress. The reoriented hydride edges measured in the RD remain in compression even after the load is removed.

Questions from Michael Preuss, University of Manchester

Q1:—You have inferred strain/stress from the change of d-spacing in the hydride. Have you also considered that the change of d-spacing could be due to a change of stoichiometry? This seems far more likely when looking at your data.

Authors' Response:—It is indeed possible that the high compressive strain measured in newly precipitated hydrides as a diffraction peak shift could be due to these initially forming hydrides having a slightly different stoichiometry than the Zr/H ratio of 1.66 typical in the δ-hydride phase. Within the δ-hydride phase, a maximum change in d-spacing due to stoichiometry of 0.002 nm could lead to a pseudo-strain of 4000 microstrain [2,3]. This cannot account for the entirety of the 10 millistrains measured and thus should not be responsible for the entire peak shift, although it could certainly be a contributing factor.

Q2:—It is very unusual that at high T during cooling, the hydrides are highly stressed while the stresses are relieved at lower temperature. Can you please comment on this?

Authors' Response:—Hydrides first nucleate as platelets and large surface energies relative to the hydride volume could induce a larger d-spacing variation than after the hydrides grow. When hydrides first nucleate, the difference in crystal structure between the hydride phase and the zirconium matrix can induce significant stresses in the nucleating hydrides. The stress relaxation observed as hydrides nucleate and grow upon cool-down could be explained by the formation of plastic dislocations in the matrix surrounding the hydrides therefore relaxing some the initial stresses. In addition, formation of new hydrides close to pre-existing hydrides (sympathetic nucleation) take advantage of the strain fields around the pre-existing hydrides and these newly precipitated hydrides could be forming with a less compressed strain state thus lowering the overall hydride population compressive strain.

Questions from Malcolm Griffiths, AECL

Q1:—For the hysteresis, how do you know that you are not seeing a kinetic effect? Is there a difference in the dissolution and precipitation rates for hydriding?

Authors' Response:—The hysteresis measured between the dissolution and precipitation temperature agrees well with previous literature determinations using differential scanning calorimetry with varying heating/cooling rates. In addition, when measuring dissolution and precipitation for various cooling rates no significant effect was measured [4]. This leads us to believe that the kinetic effect, if it present, is small.

Q2:—At the microscopic scale, what is the average spacing between all hydrides - assuming that there are finer hydrides between the coarser hydrides?

Authors' Response:—As you mention, the hydrides seen after etching are really collections of microscopic hydrides. The very small distance between these can best be investigated by TEM. Our limited TEM studies showed that the microscopic hydride platelets are stacked on top of each other and don't have measurable gaps between them [5]. For the macroscopic hydrides the average spacing depends on the hydrogen concentration

Question from Rishi Sharma, IIT Bombay, India:—You mentioned that the Zr material shows different strain behavior with the presence of reoriented hydrides than the Zr material with hydrides in as received material. Can you explain the above phenomenon?

Authors' Response:—The observed difference in strain is in the hydrides. The overall zirconium matrix strain behavior during dissolution and precipitation of hydrides is not significantly impacted by applied stress except for the stretching and compressing of the zirconium planes in the TD and the RD respectively when the tensile stress in the TD is applied. The hydride strain behavior is however very different between unstressed/not reoriented and stressed/reoriented samples. This signifies that reoriented hydrides have a different strain state than circumferential hydrides.

Question from Ted Darby, Rolls-Royce:—Do you propose an explanation for the downward shift in TSSP for reoriented hydrides? Could it simply be due to the need for these hydrides to nucleate in the matrix without the assistance of pre-existing hydrides?

Authors' Response:—The downward shift in the precipitation temperature for reoriented hydrides signifies a greater degree of undercooling is needed to precipitate radial hydrides. This suggests that stress acts to suppress circumferential hydride precipitation. In both unstressed and fully reoriented hydrides, full dissolution was achieved so no pre-existing hydrides are present when the precipitation temperature is measured. Therefore, this downward shift in Tp could be due to the difficulty of hydrides to nucleate in favorably oriented sites in the radial orientation or to the small number of these sites available in the CWSR material used in this study.

Question from R. N. Jayaraj, Dept. of Atomic Energy, India:—Hydrides get reoriented to "normal" direction under "tensile" stress. To what direction they get reoriented under compressive stress?

Authors' Response:—No experiments presented in this work have been performed under compression. However, literature results show that under sufficient compressive stress, hydrides can reorient parallel to the applied compressive stress [6].

Question from B. K. Shah, BARC Mumbai:—Different Zr alloys have different threshold stress for hydride reorientation. Please comment on the factors which are responsible for this difference.

Authors' Response:—The factors influencing the threshold stress for hydride reorientation were not investigated precisely in the work presented here. However, since the threshold stress for recrystallized material typically tends to be lower than that of cold-worked stress relieved material, influencing factors could include grain microstructure [7]. A larger fraction of grain boundaries oriented in the out of plane direction could increase hydride reorientation. Grain texture and in particular orientation of the basal poles have also been found to have a strong influence of hydride reorientation [8].

Questions from K. Somasekhar Reddy, Nuclear Fuel Complex, Hyderabad, India

Q1:—What is the necessity of more thermal cycles when all of the hydrides are dissolved in the matrix during the first thermal cycle?

Authors' Response:—As the material cools the hydrogen in solid solution is called upon to precipitate and the applied load introduces a bias for precipitation in the out of plane direction, so that depending on the cooling rate a fraction of the hydrides will reorient. Presumably a very slow cool would require only one cycle for complete reorientation.

Q2:—What is the effect of cooling rate on the reorientation of hydrides?

Authors' Response:—See the above response. Additional results on the effect of cooling rate on hydride reorientation can be found in [5].

Additional References

1. Colas, K.B., et al. *Hydride Platelet Reorientation in Zircaloy Studied with Synchrotron Radiation Diffraction. in 16th International Symposium on Zirconium in the Nuclear Industry* 2010. Chengdu, China: ASTM STP 1529, pp. 496–522.

2. Zuzek, E., et al., *H-Zr (hydrogen-zirconium): phase diagrams of binary hydrogen alloys*, A. International, Editor 2000: Ohio. p. 309–322.

3. Yamanaka, S., et al., *Characteristics of zirconium hydride and deuteride*. Journal of Alloys and Compounds, 2002. **330–332**: p. 99–104.

4. Colas, K.B., et al., *In-situ study of hydride precipitation kinetics and re-orientation in Zircaloy using synchrotron radiation*. Acta Materialia, 2010. **58**: p. 6565–6583.

5. Colas, K.B., *Fundamental Experiments on Hydride Reorientation in Zircaloy*, in Department of Nuclear Engineering, 2012, PhD Dissertation in Nuclear Engineering, The Pennsylvania State University: University Park.

6. Louthan, M.R. and R.P. Marshall, *Control of Hydride Orientation in Zircaloy*. Journal of Nuclear Materials, 1963. **9**(2): p. 170–184.

7. Bai, J., et al., *Hydride Embrittlement in Zircaloy-4 Plate, Part I Influence of Microstructure on the Hydride Embrittlement on Zircaloy-4 at 20C and 150C and Part II Interaction Between the Tensile Stress and the Hydride Morphology*. Metallurgical and Materials Transactions A, 1994. **25**.

8. Hardie, D. and M.W. Shanahan, Stress reorientation of hydrides in zirconium-2.5% niobium. Journal of Nuclear Materials, 1975. **55**(1): p. 1–13.